Self-Powered Nanosystems

DOI: 10.1002/anie.201109142

Paper-Based Supercapacitors for Self-Powered Nanosystems**

Longyan Yuan, Xu Xiao, Tianpeng Ding, Junwen Zhong, Xianghui Zhang, Yue Shen, Bin Hu, Yunhui Huang, Jun Zhou, and Zhong Lin Wang**

Owing to a tremendously increasing energy consumption of modern societies, the development of sustainable and renewable energy sources is becoming one of the most important fields of research. Green-energy sources such as solar and wind energies are both intermittent, because energy harvesting may be interrupted during night or in places where wind does not blow.[1,2] Other energy harvesting technologies such as nanogenerators could easily and efficiently convert vibration energy in living environment to electrical energy,[3,4] but they cannot continuously drive small electronics because of their limited output power.[5,6] Therefore, energy storage systems are essential for providing stable and durable output which can be regulated. Batteries and electrochemical supercapacitors are the state-of-the-art electrical energy storage systems.[1,7–9] Supercapacitors (SCs) are superior to batteries in power density, life cycles, environmental benignancy, and safety.[7,10–13]

Portable/wearable personal electronics have many future applications, which include but are not limited to wearable displays, electronic skin, and distributed sensors.[14–16] Self-powered sensor networks are likely to play key roles in the next few decades in driving the world economy.[17] The "self-powered nanotechnology" could assure sensor networks to operate independently and sustainably without a battery or at least by extending the life time of a battery.[18] Self-powered nanosystems of ultrasmall size and with multi-functionality and low energy consumption could be realized by using nanomaterials and nanofabrication technologies.[5] Here, we have fabricated all-solid-state polyaniline-based (PANI-based) flexible SCs on paper substrates as effective energy storage units for storing electric energy produced by a piezoelectric generator or a solar cell. The stored energy could be used to light up a light-emitting diode (LED) or to power a strain sensor. The results reveal the feasibility of using SCs as energy storage components in self-powered nanosystems.

Figure 1 a–c shows the fabrication process of PANI/Au/paper electrodes. Common printing papers are used as substrates, which are mainly composed of cellulose fibers, but their adhesion to metal film is weak. To solve this problem, the cellulose fibers were first coated with a thin layer of polyvinyl alcohol (PVA) film (Figure 1 a), and then an 80 nm thick Au film was evaporated onto the treated paper (Figure 1 b). The as-fabricated paper is lightweight and highly flexible, exhibiting high electrical conductivity of about 7 $\Omega\,sq^{-1}$. Furthermore, the Au/paper structure could preserve its porous structure (Figure S1 in the Supporting Information), facilitating the electrodeposition of PANI networks thereafter (Figure 1 c). A typical scanning electron microscopy (SEM) image for PANI networks is shown in Figure 1 d. PANI fibers with a diameter of about 100 nm are tangled and

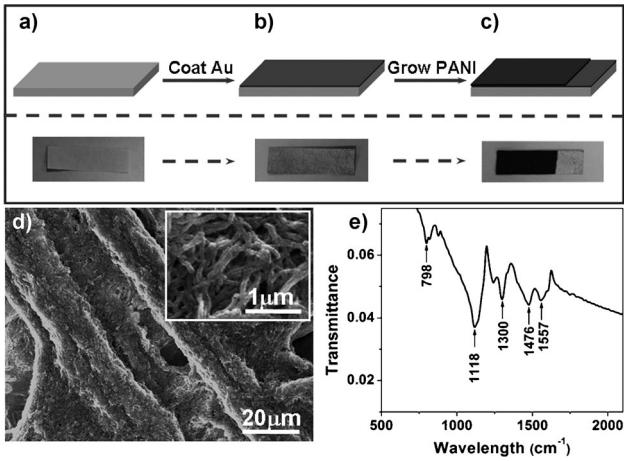

Figure 1. a–c) Fabrication procedure for PANI/Au/paper structures. d) SEM image for PANI networks on paper grown within 5 min. e) FTIR spectrum for the as-grown PANI networks.

[*] Dr. L. Y. Yuan,[+] X. Xiao,[+] T. P. Ding, J. W. Zhong, X. H. Zhang, Dr. B. Hu, Prof. J. Zhou
Wuhan National Laboratory for Optoelectronics (WNLO) and College of Optoelectronic Science and Engineering
Huazhong University of Science and Technology (HUST)
Wuhan, 430074 (China)
E-mail: jun.zhou@mail.hust.edu.cn
Dr. Y. Shen, Prof. Y. H. Huang
School of Materials Science and Engineering
Huazhong University of Science and Technology (HUST)
Wuhan, 430074 (China)
Prof. Z. L. Wang
School of Materials Science and Engineering
Georgia Institute of Technology
Atlanta, GA 30332 (USA)
E-mail: zlwang@gatech.edu
[+] These authors contributed equally to this work.

[**] This work was financially supported by the National Natural Science Foundation of China (grant number 51002056), the National Basic Research Program of China (grant number 2012CB619302), a Foundation for the Author of National Excellent Doctoral Dissertation of P.R. China (grant number 201035), the Program for New Century Excellent Talents in University (grant number NCET-10-0397), and the China Postdoctoral Science Foundation (grant number 20100480892). The authors thank the Analysis and Testing Center of Huazhong University of Science and Technology for support.

Supporting information for this article is available on the WWW under http://dx.doi.org/10.1002/anie.201109142.

© 2012 Wiley-VCH Verlag GmbH & Co. KGaA, Weinheim

twisted with each other, forming uniform and porous networks on Au-coated paper. The porous PANI networks can significantly absorb electrolyte, acting as electrolyte reservoirs to facilitate ion transport between PANI and electrolyte. PANI can hardly form networks when it is deposited at a period shorter than 2 min, while a longer deposition time of 10 or 20 min would lead to an increase of the diameter of the PANI fibers (Figure S1 in the Supporting Information). The chemical composition of the PANI networks was characterized by Fourier transform infrared spectroscopy (FTIR) and the results are shown in Figure 1e. The bands at 1557 and 1476 cm^{-1} are assigned to C=C stretching vibrations of quinoid and benzenoid rings, respectively. The band of aromatic C–N, C=N, and C–H stretching vibration at 1300, 1118, and 798 cm^{-1} can be recognized clearly, respectively.[19,20]

To evaluate the electrochemical performance of PANI networks deposited at different times, cyclic voltammetry (CV), galvanostatic charge–discharge, and electrochemical impedance spectroscopy (EIS) measurements were conducted in a three-electrode configuration in 1 M H_2SO_4 aqueous solution, and the results are given in Figure 2 and Figure S2 (see the Supporting Information). We performed CV scans of PANI networks with varying deposition times from 1 to 20 min at two different scan rates of 10 and 100 $mV s^{-1}$. The PANI mass loading is around 0.25, 0.35, 0.47, 1.0, and 2.0 mg for 1, 2, 5, 10, and 20 min of deposition time (1 cm^2), respectively. The total capacitance increases with the mass of PANI at the same scan rate, as indicated by the increases of the current density (Figure 2a and Figure S2a in the Supporting Information). As shown in Figure 2a, two couples of redox peaks, A_1/C_1 and A_2/C_2, can be attributed to redox transitions of PANI between a semiconductive state (leucoemeraldine form) and a conducting state (polaronic emeraldine form), and redox pairs such as *p*-benzo/hydroquinone and *p*-aminophenol/benzoquinoneimine, respectively.[21,22] When the scan rate increases from 10 to 100 $mV s^{-1}$, a large resistance and the RC time constant cause the curves to deteriorate from those of nearly rectangular-shape.[23] The specific capacitance with different PANI masses plotted versus the scan rates shows that the 5 min PANI networks have the highest specific capacitance (Figure S2b in the Supporting Information). CV and galvanostatic charge–discharge curves for 5 min PANI networks (0.47 mg) are shown in Figure 2b,c, respectively. As the scan rate increases, the peak current density increases but the shape deviates from that of an ideal capacitance (Figure 2b). The symmetry of the charge–discharge curves reveals the capacitive behavior of the PANI networks (Figure 2c). The impedance curves for the PANI/Au/paper electrodes show that the equivalent series resistances (ESR) are estimated to be about 7.2, 7.4, 9.8, 14.3, and 15.2 Ωcm^2 for PANI networks deposited within 1, 2, 5, 10, and 20 min, respectively (Figure 2d), which can be attributed to an increase of the PANI fiber diameter and the thickness of PANI networks with deposition time.

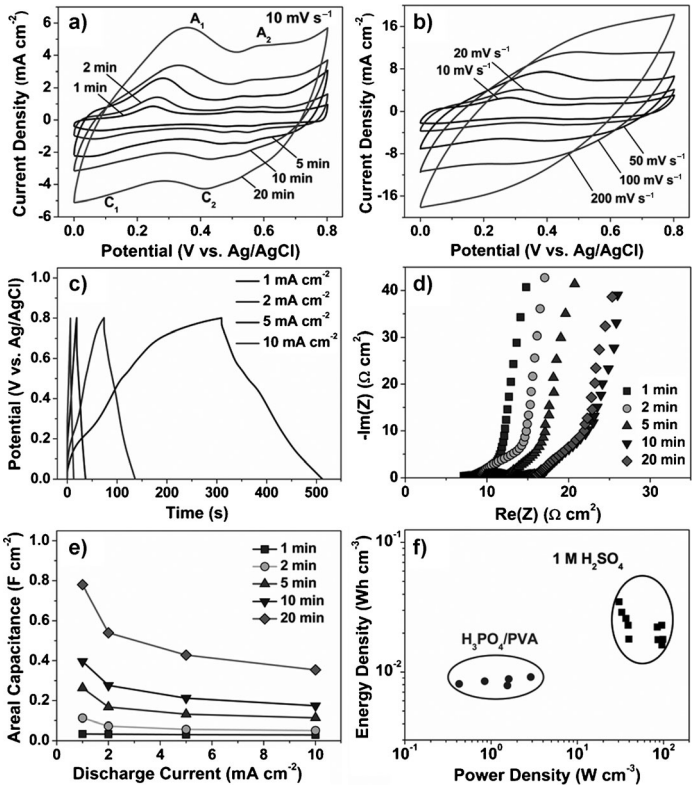

Figure 2. a) CV scans for PANI networks on Au/paper structures at a scan rate of 10 $mV s^{-1}$ with different PANI deposition times. b) CV scans for PANI networks deposited at with 5 min. c) Galvanostatic charge–discharge curves for PANI networks deposited at with 5 min. d) Nyquist plot for PANI networks obtained at different deposition times. e) Areal capacitance of PANI networks versus discharge current. f) Ragone plot for PANI networks deposited at 5 min in 1 M H_2SO_4 aqueous electrolyte and H_3PO_4/PVA solid electrolyte, respectively.

The PANI networks deposited at with 5 min exhibits the highest specific capacitance of 560 $F g^{-1}$ at a discharge current of 1 $mA cm^{-2}$ (2.13 $A g^{-1}$; Figure S2c in the Supporting Information), which is higher than that of PANI on carbon nanotubes (around 350 $F g^{-1}$).[24] In fact, the fabricated PANI networks/Au/paper electrodes are very lightweight (14 mg, 1 cm^2), therefore the capacitance per area (i.e. the areal capacitance) becomes the main concern in practical applications. The areal capacitance with respect to different PANI masses is plotted versus the discharge current in Figure 2e. The areal capacitance increases with PANI mass loading, and the 20 min PANI networks exhibit the highest areal capacitance of about 0.8 $F cm^{-2}$ and a volumetric capacitance of 800 $F cm^{-3}$ at a discharge current of 1 $mA cm^{-2}$ (0.5 $A g^{-1}$). The areal capacitance is much higher than those values reported in the literature (0.4–30 $mF cm^{-2}$) at the same discharge current density[25–28] and also the volumetric capacitance is about an order of magnitude larger than those of SCs based on carbon nanotubes and graphene (usually less than 100 $F cm^{-3}$).[29,30] The Ragone plot in Figure 2f shows that the PANI network/Au/paper electrode has the highest energy density of about 0.035 $Wh cm^{-3}$, which is about four times larger than that of activated carbon SCs (around 0.01 $Wh cm^{-3}$) and 40 times larger than that of graphene oxide (8×10^{-4} $Wh cm^{-3}$) and onion-like carbon SCs (1×10^{-3} $Wh cm^{-3}$), with a power density of

 © 2012 Wiley-VCH Verlag GmbH & Co. KGaA, Weinheim

about 100 $W cm^{-3}$ comparable to that of the mentioned SCs.[31,32]

For safety consideration and to facilitate their practical application, all-solid-state SCs are superior to their counterparts with liquid electrolytes, which need robust encapsulation to prevent leakage of liquid electrolyte and other package components making them bulky. We have assembled all-solid-state SCs with 5 min PANI networks/Au/paper electrodes using H_3PO_4/PVA electrolyte. The structure of the fabricated SCs is illustrated in Figure 3a. A 40 μm-thick H_3PO_4/PVA membrane is used as both electrolyte and separator. The weight of the device is about 60 mg, including all components of a SC. CV scans of the solid-state device show a rectangular shape at different scan rates in the range of 5 to 100 $mV s^{-1}$, indicating an ideal capacitive behavior (Figure 3b). Galvanostatic charge–discharge result of the device is shown in Figure 3c. Both the linear profile of charge-discharge curves and their symmetry reveal the good capacitive performance of the solid-state SC. In addition, the solid-state device is highly flexible (Figure 3a) and can undergo severe bending without obvious capacitive performance change (Figure 3d). As can be seen in Figure 3e, it is surprising that the all-solid-state device shows a stable areal capacitance of about 50 $mF cm^{-2}$ with respect to the discharge current increasing from 0.1 to 2 $mA cm^{-2}$ (0.2 to 4.3 $A g^{-1}$), which is superior to those of solid-state SCs reported in the literature.[24,33,34] This high-rate capability of the solid-state SCs can be attributed to their unique network structure and high electrical conductivity of PANI networks, which can allow abundant adsorption of ions, facilitating fast intercalation/de-intercalation of active species, and provide an effective path for the transport of electrons collected by Au electrodes. The all-solid-state SC shows a power density of around 3 $W cm^{-3}$ at an energy density of around 0.01 $Wh cm^{-3}$, which is even comparable to that of activated carbon SCs in aqueous electrolyte (around 0.01 $Wh cm^{-3}$).[31] EIS measurement reveals the device has an ESR of about 25 Ωcm^{-2} (Figure S3a in the Supporting Information). Furthermore, the fabricated solid SC shows long-term stability after 10000 charge–discharge cycles at 1 $mA cm^{-2}$, and Coulombic efficiency remains about 100% accordingly (Figure 3f). In addition, the fabricated SC reveals a low leakage current of about 10 μA and an open-circuit voltage of 0.3 V can retain beyond 24 h (Figure S3b in the Supporting Information).

As efficient and powerful energy storage devices, SCs could be charged and then discharge to drive various electronic components. Specially, if a sustainable and renewable energy source is used to charge SCs, they could make electronic devices work continually without a battery, forming a self-powered system.[17] We have built a system to verify the feasibility of the SCs to store energy and drive sensors, as shown in Figure 4a. A commercialized piezoelectric generator was used to harvest energy when bent back and forth by a resonator at a frequency of 3 Hz. The output voltage from the generator was first rectified by a bridge rectifier (Figure S4 in the Supporting Information), transforming alternating current (AC) to direct current (DC), and then the SCs were charged continually. The charging curve of six all-solid-state SCs

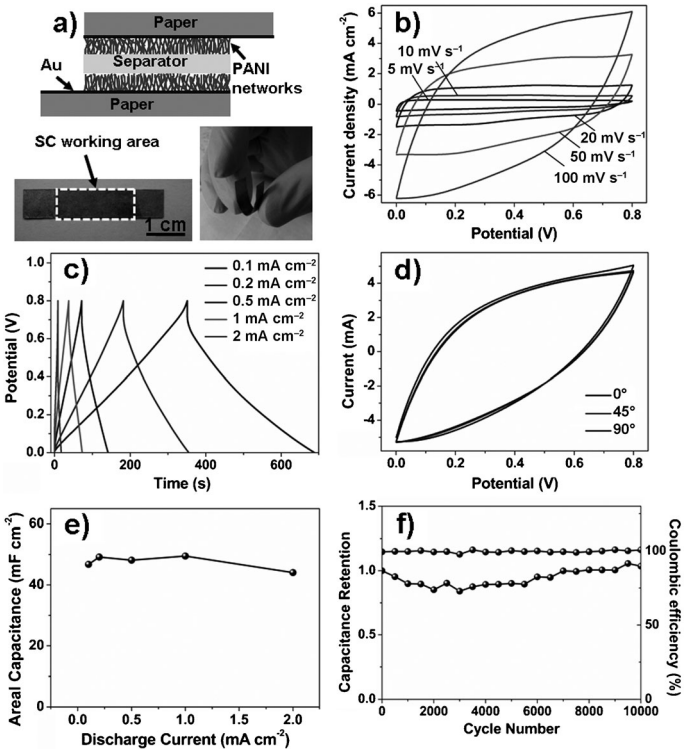

Figure 3. a) The fabricated solid-state SCs (upper) and photographs of the SC (down). b) CV and c) galvanostatic charge–discharge curves for a solid-state device with PANI networks deposited at with 5 min. d) CV scans of the all-solid-state SC at different curvature. e) Areal capacitance versus discharge current for the all-solid-state SC with PANI networks deposited at with 5 min. f) Cycle performance and Coulombic efficiency of the all-solid-state device at 1 $mA cm^{-2}$ over 10000 cycles.

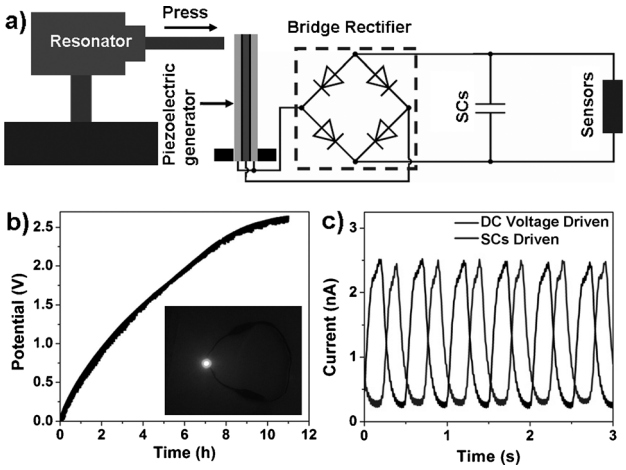

Figure 4. a) Schematic diagram of the self-powered nanosystems. b) Charging curve for six all-solid-state SCs connected in series charged by a piezoelectric generator. The inset shows an optical image of a blue LED lighted by charged SCs connected in series. c) Intensity–time curves of a strain sensor driven by DC voltage (gray curve) and SCs (black curve) for comparison.

© 2012 Wiley-VCH Verlag GmbH & Co. KGaA, Weinheim

connected in series is displayed in Figure 4b. The voltage of the SCs reached to 2.6 V after charging for 11 h by the generator (Figure S4 in the Supporting Information) since the capacitance of the SCs was quite large (around 8 mF, assuming that each capacitor has a capacitance of 50 mF) and the input current was small (around 10^{-6} A), and the charged SCs could light a blue LED (the lowest working potential is 2.5 V) for about 5 min (inset of Figure 4b). In addition, if we combine these SCs with solar cells of higher current (around 5 mA),[18] six SCs connected in series could be charged to 3.2 V quickly in 2 min (Figure S5 in the Supporting Information).

The SCs were used to power a strain sensor (the current–voltage curve is shown in Figure S6 in the Supporting Information), through which the sensor could be operated without a battery. The charged SCs were connected with a strain sensor, and the current–time (*I–t*) curve of the system was measured under cyclically straining introduced to the sensor at a frequency of 2 Hz (Figure 4c). The current reached the same value in each cycle of straining and fully recovered to the state without strain, indicating that the output voltage of SCs was steady. Remarkably, the response of the sensor driven by either a DC voltage of 0.3 V or SCs in series shows no distinct difference. This demonstration implies that the self-powered nanosystem has the potential for applications in reliably driving mobile sensors and devices.

In summary, we have successfully fabricated highly flexible and high-performance all-solid-state SCs based on PANI/Au/paper structures. The fabrication procedure is simple and could be easily scaled-up to large-scale production. The solid-state SCs show a high energy density of around 0.01 Wh cm^{-3} and a power density of around 3 W cm^{-3}. A potential application of the flexible solid-state SC in self-powered nanosystems is also shown, which opens up new ways for the use of SCs.

Experimental Section

Preparation of PANI/Au/Paper Electrodes: All chemicals were analytical grade and were used without further purification. A PVA powder was mixed with deionized water (1 g of PVA per 10 mL of H_2O). The whole mixture was heated up steadily to around 85 °C under vigorous stirring until the solution became clear. Then the solution cooled down to room temperature. A piece of printing paper was immersed into the PVA solution until PVA penetrated the paper thoroughly. After that, the treated paper was left in the fume hood at room temperature for 12 h to vaporize the excess water. A thin film of gold (80 nm) was deposited on the treated papers by a E-beam Evaporation System (EB-500S, Alpha plus, Korea). The PANI nanowires were synthesized by oxidation of aniline (0.3 M in 1 M HCl) through a two-step method on a conventional three-electrode system.[35] For the first step of the nucleation of PANI, a constant potential of 0.8 V was applied for 1 min at room temperature. After that, the nanowires were grown under constant current conditions of 2 mA cm^{-2}.

Preparation of the flexible all-solid-state SCs: A H_3PO_4/PVA gel electrolyte was simply prepared by mixing PVA powder (6 g), H_3PO_4 (6 g) and deionized water (60 mL) together. Then the mixture was heated to around 85 °C under vigorous stirring until the solution became clear. After cooling down, two PANI/Au/paper electrodes were immersed for 5 min, taken out, and then assembled into a thin H_3PO_4/PVA gel membrane which worked as both the solid electrolyte and separator. The device was left in the fume hood at room temperature to vaporize the excess water.

Characterization: The morphology of the samples was probed by high-resolution field emission scanning electron microscopy (FEI Sirion 200). Fourier transform infrared spectra were recorded on a Bruker, Equinox 55 spectrometer. The electrochemical measurements were all carried out at room temperature using Autolab PGSTAT302N. For the aqueous electrolyte test, a part of the PANI/Au/paper electrode (around 0.7 cm × 1.5 cm) was dipped in the 1 M H_2SO_4 aqueous solution and used as the working electrode. An Ag/AgCl reference electrode and a carbon rod counter electrode were used for the measurement. The all-solid-state SC devices (with a size of around 0.7 cm × 1.5 cm) were tested under highly flexible conditions. For the self-powered measurement, a piezoelectric generator (PL112·PL140 PICMA®, USA) was fixed by two home-made three-dimension mechanical stages and impelled by a resonator (JZK, SINOCERA, China) which was driven by a swept signal generator (YE 1311-D, SINOCERA, China). A low-noise voltage preamplifier (Model SR560, STANFORD RESEARCH SYSTEMS, USA) and a low-noise current preamplifier (Model SR570, STANFORD RESEARCH SYSTEMS, USA) were used to measure the voltage—time and intensity–time curves. In videos, a multimeter (Agilent U1252A) was used to measure the voltage in real-time.

Received: December 25, 2011
Published online: April 3, 2012

Keywords: paper substrates · polymers · self-powered nanosystems · supercapacitors

[1] P. Simon, Y. Gogotsi, *Nat. Mater.* **2008**, *7*, 845 – 854.
[2] B. Z. Tian, X. L. Zheng, T. J. Kempa, Y. Fang, N. F. Yu, G. H. Yu, J. L. Huang, C. M. Lieber, *Nature* **2007**, *449*, 885 – 890.
[3] Z. L. Wang, J. H. Song, *Science* **2006**, *312*, 242 – 246.
[4] R. S. Yang, Y. Qin, L. M. Dai, Z. L. Wang, *Nat. Nanotechnol.* **2009**, *4*, 34 – 39.
[5] S. Xu, B. J. Hansen, Z. L. Wang, *Nat. Commun.* **2010**, *1*, 93.
[6] G. Zhu, R. Yang, S. Wang, Z. L. Wang, *Nano Lett.* **2010**, *10*, 3151 – 3155.
[7] J. M. Miller, B. Dunn, T. D. Tran, R. W. Pekala, *J. Electrochem. Soc.* **1997**, *144*, L309 – L311.
[8] P. Poizot, S. Laruelle, S. Grugeon, L. Dupont, J. M. Tarascon, *Nature* **2000**, *407*, 496 – 499.
[9] J. M. Tarascon, M. Armand, *Nature* **2001**, *414*, 359 – 367.
[10] B. E. Conway, *Electrochemical Supercapacitors*: *Scientific*, *Fundamentals and Technological Applications*, Plenum, New York, **1999**, pp. 29 – 30.
[11] E. Frackowiak, F. Beguin, *Carbon* **2001**, *39*, 937 – 950.
[12] R. Kötz, M. Carlen, *Electrochim. Acta* **2000**, *45*, 2483 – 2498.
[13] J. R. Miller, P. Simon, *Science* **2008**, *321*, 651 – 652.
[14] J. A. Rogers, Y. G. Huang, *Proc. Natl. Acad. Sci. USA* **2009**, *106*, 10875 – 10876.
[15] L. Y. Yuan, J. J. Dai, X. H. Fan, T. Song, Y. T. Tao, K. Wang, Z. Xu, J. Zhang, X. D. Bai, P. X. Lu, J. Chen, J. Zhou, Z. L. Wang, *ACS Nano* **2011**, *5*, 4007 – 4013.
[16] L. Y. Yuan, Y. T. Tao, J. Chen, J. J. Dai, T. Song, M. Y. Ruan, Z. W. Ma, L. Gong, K. Liu, X. H. Zhang, X. J. Hu, J. Zhou, Z. L. Wang, *Adv. Funct. Mater.* **2011**, *21*, 2150 – 2154.
[17] Z. L. Wang, *Nano Today* **2010**, *5*, 512 – 514.
[18] X. Xiao, L. Y. Yuan, J. W. Zhong, T. P. Ding, Y. Liu, Z. X. Cai, Y. G. Rong, H. W. Han, J. Zhou, Z. L. Wang, *Adv. Mater.* **2011**, *23*, 5440 – 5444.
[19] Z. X. Wei, M. X. Wan, *Adv. Mater.* **2002**, *14*, 1314 – 1317.
[20] Y. Yang, W. Yang, *Polym. Adv. Technol.* **2005**, *16*, 24 – 31.

 © 2012 Wiley-VCH Verlag GmbH & Co. KGaA, Weinheim

[21] D. W. Wang, F. Li, J. P. Zhao, W. C. Ren, Z. G. Chen, J. Tan, Z. S. Wu, I. Gentle, G. Q. Lu, H. M. Cheng, *ACS Nano* **2009**, *3*, 1745 – 1752.
[22] D. E. Stilwell, S. M. Park, *J. Electrochem. Soc.* **1988**, *135*, 2254 – 2262.
[23] L. Hu, W. Chen, X. Xie, N. Liu, Y. Yang, H. Wu, Y. Yao, M. Pasta, H. N. Alshareef, Y. Cui, *ACS Nano* **2011**, *5*, 8904 – 8913.
[24] C. Meng, C. Liu, L. Chen, C. Hu, S. Fan, *Nano Lett.* **2010**, *10*, 4025 – 4031.
[25] J. Bae, M. K. Song, Y. J. Park, J. M. Kim, M. Liu, Z. L. Wang, *Angew. Chem.* **2011**, *123*, 1721 – 1725; *Angew. Chem. Int. Ed.* **2011**, *50*, 1683 – 1687.
[26] H. J. In, S. Kumar, Y. Shao-Horn, G. Barbastathis, *Appl. Phys. Lett.* **2006**, *88*, 083104.
[27] M. Kaempgen, C. K. Chan, J. Ma, Y. Cui, G. Gruner, *Nano Lett.* **2009**, *9*, 1872 – 1876.
[28] M. Pasta, F. La Mantia, L. B. Hu, H. D. Deshazer, Y. Cui, *Nano Res.* **2010**, *3*, 452 – 458.
[29] D. N. Futaba, K. Hata, T. Yamada, T. Hiraoka, Y. Hayamizu, Y. Kakudate, O. Tanaike, H. Hatori, M. Yumura, S. Iijima, *Nat. Mater.* **2006**, *5*, 987 – 994.
[30] C. Emmenegger, P. Mauron, P. Sudan, P. Wenger, V. Hermann, R. Gallay, A. Züttel, *J. Power Sources* **2003**, *124*, 321 – 329.
[31] D. Pech, M. Brunet, H. Durou, P. Huang, V. Mochalin, Y. Gogotsi, P. L. Taberna, P. Simon, *Nat. Nanotechnol.* **2010**, *5*, 651 – 654.
[32] W. Gao, N. Singh, L. Song, Z. Liu, A. L. M. Reddy, L. Ci, R. Vajtai, Q. Zhang, B. Wei, P. M. Ajayan, *Nat. Nanotechnol.* **2011**, *6*, 496 – 500.
[33] L. Y. Yuan, X. H. Lu, X. Xiao, T. Zhai, J. J. Dai, F. C. Zhang, B. Hu, X. Wang, L. Gong, J. Chen, C. G. Hu, Y. X. Tong, J. Zhou, Z. L. Wang, *ACS Nano* **2012**, *6*, 656 – 661.
[34] B. G. Choi, J. Hong, W. H. Hong, P. T. Hammond, H. Park, *ACS Nano* **2011**, *5*, 7205 – 7213.
[35] Q. Cheng, J. Tang, J. Ma, H. Zhang, N. Shinya, L. C. Qin, *J. Phys. Chem. C* **2011**, *115*, 23584 – 23590.

 © 2012 Wiley-VCH Verlag GmbH & Co. KGaA, Weinheim